Thermochemical scanning probe lithography of protein gradients at the nanoscale

E. Albisetti,[1,2] K. M. Carroll,[2,5] X. Lu,[2] J. E. Curtis,[2] D. Petti,[1] R. Bertacco,[1,3] E. Riedo[2,4]

[1] Dipartimento di Fisica, Politecnico di Milano, 20133 Milano, Italy.
[2] School of Physics, Georgia Institute of Technology, Atlanta, GA 30332, USA.
[3] IFN-CNR, c/o Politecnico di Milano, Piazza Leonardo da Vinci, 32, 20133 Milano, Italy.
[4] CUNY-Advanced Science Research Center and City College New York, City University of New York, 85 St Nicholas Terrace, New York, New York 10031, USA.

E-mail: edoardo.albisetti@polimi.it; elisa.riedo@asrc.cuny.edu

Abstract

Patterning nanoscale protein gradients is crucial for studying a variety of cellular processes *in-vitro*. Despite the recent development in nanofabrication technology, combining sub-micrometric resolution and fine control of protein concentrations is still an open challenge. Here, we demonstrate the use of thermochemical scanning probe lithography (tc-SPL) for defining micro- and nano-sized patterns with precisely controlled protein concentration. First, tc-SPL is performed by scanning a heatable atomic force microscopy tip on a polymeric substrate, for locally exposing reactive amino groups on the surface, then the substrate is functionalized with streptavidin and laminin proteins. We show, by fluorescence microscopy on the patterned gradients, that it is possible to precisely tune the concentration of the immobilized proteins by varying the patterning parameters during tc-SPL. This paves the way to the use of tc-SPL for defining sub-micrometric protein gradients to be used as chemical cues for studying and regulating cellular processes *in-vitro*.

Introduction

Controlled distributions of extracellular matrix proteins (ECM) are known to regulate *in-vivo* a variety of cellular mechanisms such as growth, migration and differentiation [1–5]. For example, during the nervous system development, gradients of ECM proteins, such as laminins, are responsible for the cell adhesion to the ECM and guide neurite outgrowth and axonal elongation [6–9]. The study and control of such processes necessarily rely on the fabrication of *in-vitro* models mimicking the complexity of the extracellular environment.

With this goal, several biopatterning techniques have been developed during the past decades, including microdispensing techniques [10] and microfluidic systems [11], optical lithography [12,13], photochemical patterning [14–16]. Nowadays, the most common technique is microcontact printing [17–20], which involves the creation of a stamp by soft-lithography from a microfabricated mold, and the subsequent transfer of molecules

[5] Current address: IBM Research - Zurich, 8803 Rueschlikon, Switzerland.

from the stamp to the final substrate with a fast and inexpensive printing process. Nano-shaving, an AFM-based technique was also used for defining protein patterns [21]; however, it does not allow a straightforward control over the concentration of the immobilized molecules. A wide variety of microfluidic devices also in combination with grayscale soft-lithographic techniques were employed for generating protein gradients [22,23]; however, their resolution and versatility are limited and their complexity usually prevents them from being widely employed. Laser assisted photobleaching was successfully employed for creating gradients of ECM proteins [24], but its resolution is limited by the diffraction of the laser beam. E-Beam lithography is a viable alternative for generating protein nanopatterns, but it requires suitable conductive substrates and the use of a cleanroom [25]. As shown, despite the recent developments in micro- and nano-fabrication technology enabled a plethora of methods for defining protein patterns, combining nanoscale resolution and precise control over the protein concentration is still an open challenge.

Thermally-assisted scanning probe lithography is based on the use of a heated AFM tip to locally induce physico-chemical modifications on the surface of a suitable substrate [26–30]. Recently, some of the authors showed that tc-SPL can be used for creating nanopatterns of reactive amino groups suitable for the immobilization of proteins [31], and that it is possible to control the concentration of such amino groups with extreme precision by tuning the patterning parameters [32,33].

In this paper we demonstrate the creation by tc-SPL of arbitrarily shaped micro- and sub-micrometric patterns of controlled graded concentration of streptavidin and laminin proteins. First, controlled concentrations of reactive amino groups were exposed by tc-SPL. Subsequently the surface was selectively functionalized with streptavidin and laminin by exploiting the biotin-streptavidin complex in the bridge configuration [34]. Finally, the patterns were visualized via fluorescence microscopy. This work paves the way to the use of tc-SPL for defining nano-scale protein gradients for regulating and studying cellular processes in *in-vitro* cellular networks.

Materials and Methods

Thermochemical nanopatterning

tc-SPL patterning was performed on polymer coated Si substrates employing a modified Agilent 5500 scanning probe microscope. The methacrylate copolymer used for patterning presents functional amines (-NH_2) which are protected by tetrahydropyran (THP) carbamate groups [31]. Upon heating the surface around the deprotection temperature T_d ~200°C, the protecting groups dissociate, unmasking the primary amines. Local deprotection of the polymer surface was achieved by sweeping a resistively heatable Si tip [35] in contact mode on the sample surface, while controlling the tip temperature, load and velocity. In particular, in this work the surface concentration of the exposed amine groups was controlled by varying the tip temperature during scanning, while maintaining a constant tip velocity of 12 μm/s and load. During patterning, the heater power P_H, which is related to the tip temperature at the tip-sample interface, was recorded. When patterning the square-shaped structures, the tip was swept in a zig-zag fashion keeping a 125 nm distance between each line. At the end of each line, the tip was lifted from the surface and heated to clean and remove residues of the polymer. AFM visualization of the patterns was performed by scanning the sample surface with the same tip in contact mode.

Surface functionalization and fluorescence microscopy

The immobilization of laminin on tc-SPL patterns was achieved by employing the biotin-streptavidin bridge configuration, where a streptavidin molecule serves as a link between two biotinylated species. The high affinity and specificity of the biotin-streptavidin interaction allows the use of low concentrations of reagents and short reaction times, which in turn give rise to a low non-specific binding. First, NHS-biotin was bound to the tc-SPL patterns by incubating the patterned surface for 1 h with a 1 μM NHS-biotin solution in dimethyl-sulfoxide (DMSO). NHS-activated biotins react efficiently with primary amino groups (-NH2) on the patterned surface in alkaline buffers to form stable amide bonds. After incubation, the surface was washed repeatedly with de-ionized water (DI-H_2O) and phosphate buffer solution (PBS). The surface was incubated for 30 min with a 100 nM DyLight® 633-streptavidin solution in PBS. The DyLight® 633 fluorophore, which emits in the red, allows visualization of the streptavidin patterns by fluorescence microscopy. After incubation, the surface was washed repeatedly with DI-H_2O and PBS. A 40 nM solution of biotinylated laminin solution in PBS was incubated for 30 min. The Laminin-1 from Engelbreth-Holm-Swarm (EHS) mouse tumor tissue (MW ~ 850 kDa), already biotinylated, was purchased by Cytoskeleton, Inc.®. After the incubation, the surface was washed with DI-H_2O and PBS. Laminin was visualized through immunofluorescence by incubating the surface with Sigma Rabbit Anti-Laminin primary antibody (1:160 dilution in PBS, 1% BSA) for 1 h, and subsequently with Sigma Anti-Rabbit FITC conjugated secondary antibody (1:50 dilution in PBS, 1% BSA), for 45 min.
Fluorescence imaging was performed using epifluorescence microscopy on an inverted Nikon TE2000 microscope equipped with a Nikon Intensilight for illumination and a Roper Scientific CoolSnap CCD camera. Images were obtained using a 40× 1.3 NA oil immersed objective.

Results and discussion

In Fig. 1, the steps of the functionalization process are shown. First, tc-SPL was performed on the pristine polymer coated surface (panel a), for locally exposing a controlled concentration of amino groups (panel b). The patterns are visible both in the topography, shown in the inset of panel b, and in the friction image (not shown). In the first case, the height of the square pattern is related to the quantity of polymer removed due to the chemical deprotection process, which is determined by the heating temperature [32]. In the second case, the amino groups exposed produce an increase in the hydrophilicity of the polymer which, in turn, produces larger friction forces at the nanoscale due to larger capillary forces. [31] The inset in Fig. 1 (b) shows the topography image of a 3 x 4 array of 5 x 5 μm^2 squares, patterned increasing the heater power, indicated in white for each square. After patterning, the surface was incubated with NHS-biotin, panel (c), and subsequently with fluorescent streptavidin, panel (d), following the protocols described in the above section. The immobilized streptavidin acts as a bridge for the subsequent immobilization of biotinylated biomolecules, such as laminin in our case, panel (e). For allowing the visualization of the immobilized laminin, the surface was further incubated with anti-laminin primary antibody and subsequently with the fluorescent secondary antibody.

In order to demonstrate the versatility of tc-SPL for defining arbitrarily shaped micro- and sub-micrometric patterns with controlled protein concentration, we patterned arrays of squares (Fig. 2 (a)), triangles (Fig. 2 (b)), and single lines (Fig. 2 (c) and Fig. 2 (d)) with different heating powers, and subsequently functionalized the surface with fluorescent streptavidin following the procedure described above.

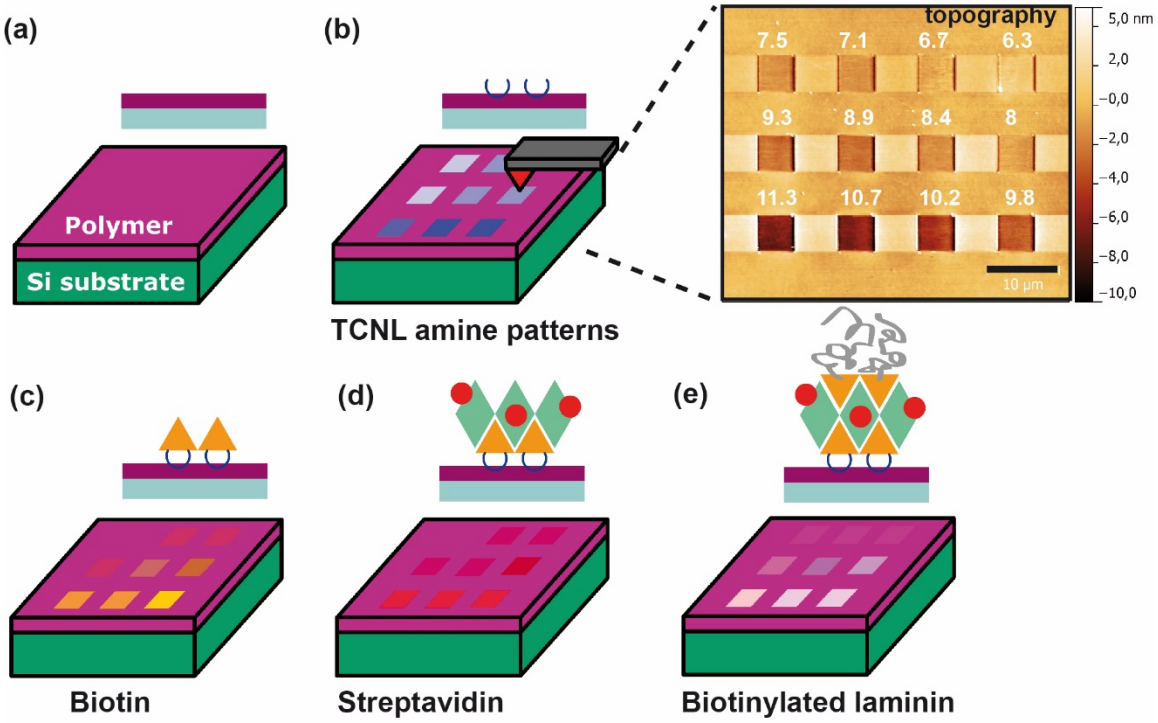

Fig. 1 Sketch of the patterning process and surface functionalization with laminin. (a) Pristine polymer/Si surface. (b) Controlled concentrations of amino groups are exposed on the polymer surface by tc-SPL. In the inset: topography image of an array of squares patterned at different heating power (in mW). Scale bar = 10 µm. (c) Amino reactive biotin is immobilized on the amine patterns. (d) Fluorescent streptavidin binds to biotinylated patterns. (e) Biotinylated laminin binds to the streptavidin in the biotin-streptavidin-biotin bridge configuration.

Fig. 2 (a) shows a 3 x 4 array of 6 x 6 μm^2 squares. For each square, the heater power in mW used for patterning is indicated. The low dye concentration ensures an approximately linear relationship between the fluorescence intensity and the concentration of immobilized streptavidin. The fluorescence intensity increases monotonically with the heater power (i.e. with the interface temperature), reaching a maximum around 9.6 mW. If higher temperatures are applied, the polymer starts to show signs of decomposition, and thus a decrease in the intensity signal due to the reduced binding is observed, consistently with what observed in Ref. [32]. Fig. 2 (b) shows the fluorescence intensity of arrays of triangular shapes patterned employing a uniform heating power around 10 mW. Fig. 2 (c) and (d) show the streptavidin fluorescence intensity of extensive tc-SPL patterns produced by 60 µm long single vertical lines separated by 500 nm (c) and 2 µm (d). The heater voltage was kept constant along the vertical lines and increased linearly from left to right, thus producing the intensity gradient shown. The uniformity

in the fluorescent intensity along the vertical direction in panel (c), and (d) shows that it is possible to combine a precise control over the nanoscale protein concentration, with a remarkable uniformity over large areas.
Panel (e) shows the average intensity profile extracted by panel (c), as a function of the heater power. The curve obtained shows the approximately linear relation between the concentration of immobilized streptavidin and the heating power in the 7 mW – 9mW range. This feature, which derives from the linear relation between the concentration of the amines exposed by tc-SPL and the heating power, is particularly appealing because it allows a straightforward control of the immobilized protein concentration.

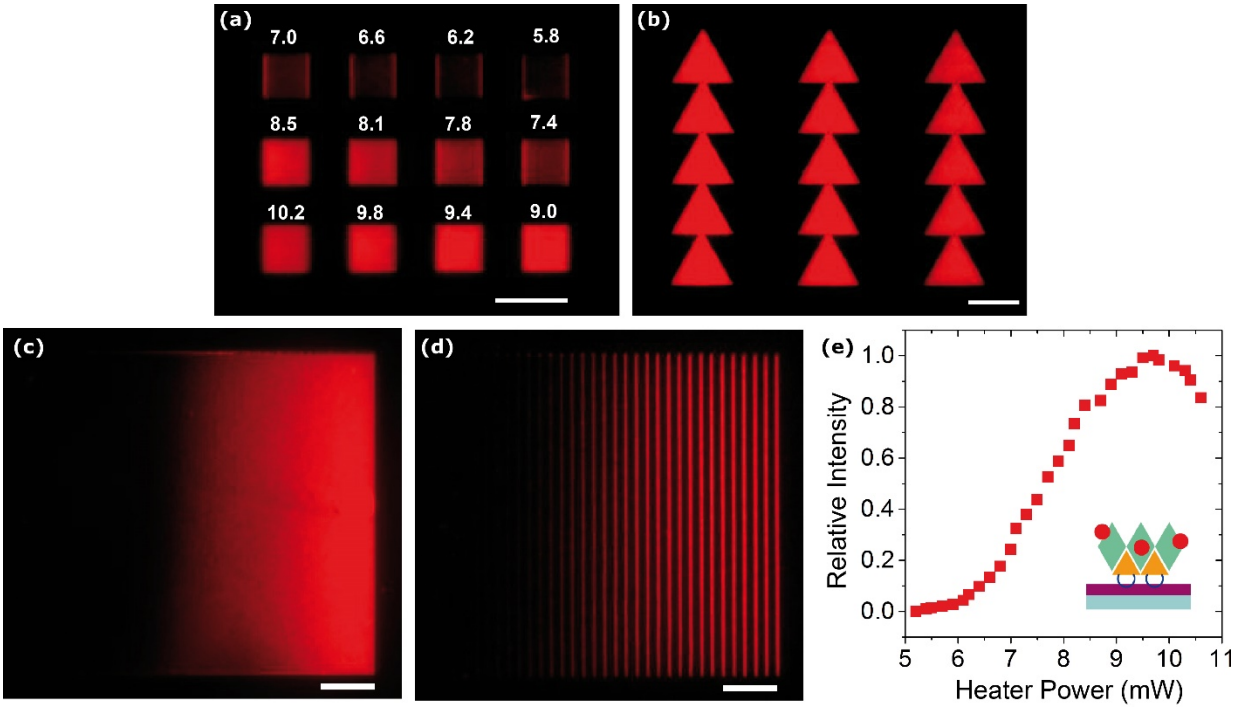

Fig. 2 (a) Fluorescence image of DyLight® 633-streptavidin immobilized upon an array of squares, patterned at different heating powers (in mW), and triangular shapes (b) patterned with a 10 mW heating power. (c), (d) Fluorescence images from the DyLight® 633-streptavidin in case of 60 μm long patterned lines with separation of 500 nm and 2 μm, respectively. The heater voltage was increased linearly from left to right. (e) Fluorescence intensity profile from panel (d) as a function of the heater power. Scale bars = 10 μm.

Fig. 3 shows our results on the patterning of protein gradients. Patterns with graded protein concentration are obtained by varying the heating power during the scan. Panel (a) and (b) shows the fluorescence images of a tc-SPL pattern consisting of four 10 x 10 μm^2 squares connected by 2 μm wide stripes. In panel (a), white numbers indicate the heating power in mW used for patterning each square. The heater voltage was varied linearly when patterning the connecting stripes, so that a gradient in the amines exposed on the surface of the polymer was created. Panel (a) shows the red fluorescence from the streptavidin, while panel (b) shows the green fluorescence from the secondary antibody, whose intensity is proportional to the concentration of immobilized laminin. Panel (c) shows the profile of the two intensities (along dashed lines in panels (a) and (b)), plotted as a function of the

distance from the left square (*x*-position). The intensities were normalized to the average of their values at $x = 0$ μm and at $x = 39$ μm. The linear decrease in the fluorescence intensities observed up to $x = 20$ μm, and the smooth decay observed from $x = 20$ μm up to $x = 37$ μm are consistent with Fig. 2 (e). The fact that the two profiles overlap indicates that the concentration of immobilized streptavidin is reflected in the concentration of the immobilized laminin, and confirms that the binding mechanism of laminin is the interaction between biotin and streptavidin in the bridge configuration. This demonstrates that by using tc-SPL generated amine gradients it is possible to control in a straightforward way the concentration of immobilized proteins and thus produce complex spatial gradients.

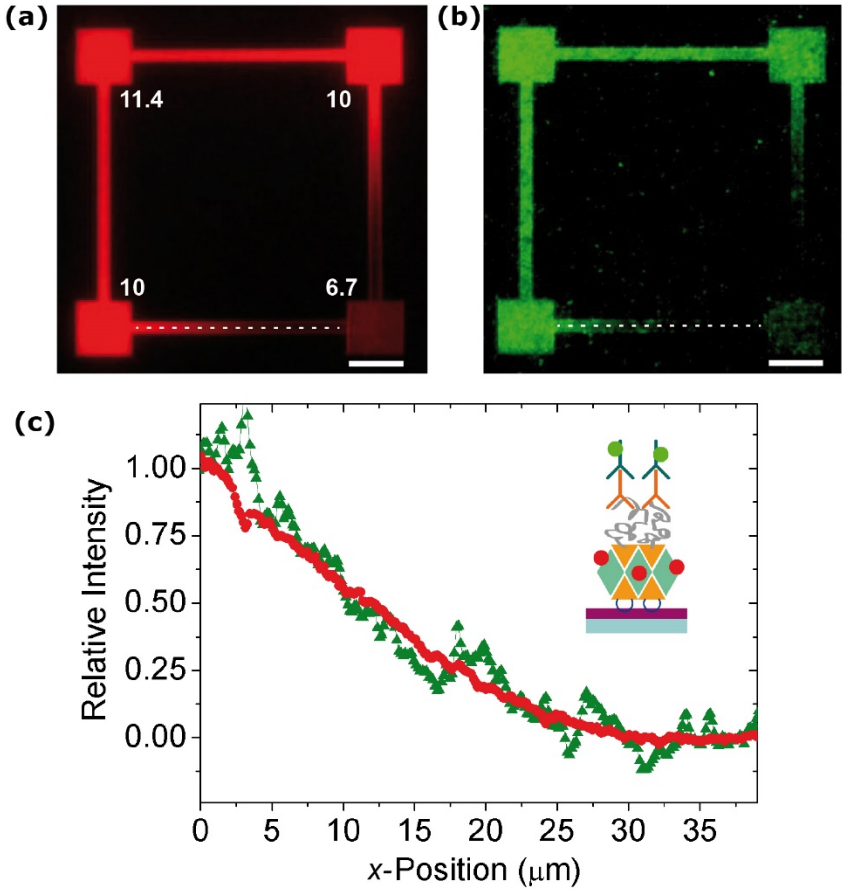

Fig. 3 (a) Fluorescence image from the DyLight® 633-streptavidin and heater power of the squares in mW. (b) Fluorescence image from laminin, visualized through the FITC-Sigma Anti-Rabbit secondary antibody. The heating voltage is constant within the squares, and varied linearly in the connections, giving rise to a concentration gradient in the exposed amines. (c) Intensity profiles along the dashed line in panels (a) and (b). Scale bars = 10 μm.

Conclusion

In this paper, we demonstrated the nanopatterning of protein gradients via thermochemical scanning probe lithography. By varying the temperature of the heatable AFM tip during tc-SPL, we exposed controlled

concentrations of amino groups on the sample surface. Such fine tuning of the concentration of the exposed amines was employed for immobilizing gradients of streptavidin and laminin proteins exploiting the biotin-streptavidin complex. We demonstrated that tc-SPL allows to generate micro- and sub-micrometric protein patterns combining the high resolution of scanning probe lithography with a straightforward control of the concentration of the immobilized biomolecules. High-speed patterning of large areas can be achieved by parallelizing tc-SPL as demonstrated in Ref. [36]. The combination of such features is particularly appealing for studying and exploiting *in-vitro* the interaction of cells with nanoscale chemical cues, e.g. for the development of neural networks, and the study of cell adhesion and differentiation via the nanopatterning of ECM proteins.

Acknowledgments

E.R. acknowledges partial support from the National Science Foundation (NSF; grant no. CMMI 1436375). E.A., D.P. and R.B. acknowledge support from Fondazione Cariplo via Project UMANA (2013-0735). J.E.C and K.M.C. acknowledge support from the National Science Foundation (NSF; grant no. PHYS 0848797 and PHYS 1205878).

References

[1] Huh D, Matthews B D, Mammoto A, Montoya-Zavala M, Hsin H Y and Ingber D E 2010 Reconstituting Organ-Level Lung Functions on a Chip *Science* **328** 1662–8

[2] Kim D H, Lee H, Lee Y K, Nam J M and Levchenko A 2010 Biomimetic nanopatterns as enabling tools for analysis and control of live cells *Adv. Mater.* **22** 4551–66

[3] Biggs M J P, Richards R G and Dalby M J 2010 Nanotopographical modification: A regulator of cellular function through focal adhesions *Nanomedicine Nanotechnology, Biol. Med.* **6** 619–33

[4] Kim D H, Provenzano P P, Smith C L and Levchenko A 2012 Matrix nanotopography as a regulator of cell function *J. Cell Biol.* **197** 351–60

[5] Bonnans C, Chou J and Werb Z 2014 Remodelling the extracellular matrix in development and disease *Nat. Rev. Mol. Cell Biol.* **15** 786–801

[6] Lauffenburger D A and Horwitz A F 1996 Cell Migration: A Physically Integrated Molecular Process *Cell* **84** 359–69

[7] Parent C A and Devreotes P N 1999 A Cell's Sense of Direction *Science* **284** 765–70

[8] Tessier-Lavigne M and Goodman C S 1996 The Molecular Biology of Axon Guidance *Science* **274** 1123–33

[9] Song H and Poo M 2001 The cell biology of neuronal navigation. *Nat. Cell Biol.* **3** E81–8

[10] Gustavsson P, Johansson F, Kanje M, Wallman L and Linsmeier C E 2007 Neurite guidance on protein micropatterns generated by a piezoelectric microdispenser. *Biomaterials* **28** 1141–51

[11] Martinoia S, Bove M, Tedesco M, Margesin B and Grattarola M 1999 A simple microfluidic system for patterning populations of neurons on silicon micromachined substrates *J. Neurosci. Methods* **87** 35–44

[12] Sorribas H, Padeste C and Tiefenauer L 2002 Photolithographic generation of protein micropatterns for neuron culture applications. *Biomaterials* **23** 893–900

[13] Albisetti E, Petti D, Damin F, Cretich M, Torti A, Chiari M and Bertacco R 2014 Photolithographic bio-

patterning of magnetic sensors for biomolecular recognition *Sensors Actuators B Chem.* **200** 39–46

[14] Nicolau D V, Taguchi T, Taniguchi H, Tanigawa H and Yoshikawa S 1999 Patterning neuronal and glia cells on light-assisted functionalised photoresists. *Biosens. Bioelectron.* **14** 317–25

[15] Clémence J F, Ranieri J P, Aebischer P and Sigrist H Photoimmobilization of a bioactive laminin fragment and pattern-guided selective neuronal cell attachment. *Bioconjug. Chem.* **6** 411–7

[16] Scrimgeour J, Kodali V K, Kovari D T and Curtis J E 2010 Photobleaching-activated micropatterning on self-assembled monolayers *J. Phys. Condens. Matter* **22** 194103

[17] Offenhausser A, Bocker-Meffert S, Decker T, Helpenstein R and Gasteier P 2007 Microcontact printing of proteins for neuronal cell guidance *Soft Matter* **3** 290

[18] Agheli H, Malmström J, Larsson E M, Textor M and Sutherland D S 2006 Large area protein nanopatterning for biological applications. *Nano Lett.* **6** 1165–71

[19] Sun Y, Jallerat Q, Szymanski J M and Feinberg A W 2015 Conformal nanopatterning of extracellular matrix proteins onto topographically complex surfaces. *Nat. Methods* **12** 134–6

[20] Castagna R, Bertucci A, Prasetyanto E A, Monticelli M, Conca D V, Massetti M, Sharma P P, Damin F, Chiari M, De Cola L and Bertacco R 2016 Reactive Microcontact Printing of DNA Probes on (DMA-NAS-MAPS) Copolymer-Coated Substrates for Efficient Hybridization Platforms *Langmuir* **32** 3308–13

[21] Staii C, Viesselmann C, Ballweg J, Shi L, Liu G, Williams J C, Dent E W, Coppersmith S N and Eriksson M a 2009 Positioning and guidance of neurons on gold surfaces by directed assembly of proteins using Atomic Force Microscopy. *Biomaterials* **30** 3397–404

[22] Millet L J, Stewart M E, Nuzzo R G and Gillette M U 2010 Guiding neuron development with planar surface gradients of substrate cues deposited using microfluidic devices. *Lab Chip* **10** 1525–35

[23] Bowen A M, Ritchey J a, Moore J S and Nuzzo R G 2011 Programmable chemical gradient patterns by soft grayscale lithography. *Small* **7** 3350–62

[24] Bélisle J M, Correia J P, Wiseman P W, Kennedy T E and Costantino S 2008 Patterning protein concentration using laser-assisted adsorption by photobleaching, LAPAP. *Lab Chip* **8** 2164–7

[25] Horzum U, Ozdil B and Pesen-Okvur D 2015 Differentiation of Normal and Cancer Cell Adhesion on Custom Designed Protein Nanopatterns *Nano Lett.* **15** 5393–403

[26] Szoszkiewicz R, Okada T, Jones S C, Li T-D, King W P, Marder S R and Riedo E 2007 High-speed, sub-15 nm feature size thermochemical nanolithography. *Nano Lett.* **7** 1064–9

[27] Kim S, Bastani Y, Lu H, King W P, Marder S, Sandhage K H, Gruverman A, Riedo E and Bassiri-Gharb N 2011 Direct Fabrication of Arbitrary-Shaped Ferroelectric Nanostructures on Plastic, Glass, and Silicon Substrates. *Adv. Mater.* **23** 3786–90

[28] Wei Z, Wang D, Kim S, Kim S-Y, Hu Y, Yakes M K, Laracuente A R, Dai Z, Marder S R, Berger C, King W P, de Heer W a, Sheehan P E and Riedo E 2010 Nanoscale tunable reduction of graphene oxide for graphene electronics. *Science* **328** 1373–6

[29] Garcia R, Knoll A W and Riedo E 2014 Advanced scanning probe lithography. *Nat. Nanotechnol.* **9** 577–87

[30] Albisetti E, Petti D, Pancaldi M, Madami M, Tacchi S, Curtis J, King W P, Papp A, Csaba G, Porod W, Vavassori P, Riedo E and Bertacco R 2016 Nanopatterning reconfigurable magnetic landscapes via thermally assisted scanning probe lithography. *Nat. Nanotechnol.* DOI: 10.1038/nnano.2016.25

[31] Wang D, Kodali V K, Underwood II W D, Jarvholm J E, Okada T, Jones S C, Rumi M, Dai Z, King W P, Marder S R, Curtis J E and Riedo E 2009 Thermochemical Nanolithography of Multifunctional Nanotemplates for Assembling Nano-Objects *Adv. Funct. Mater.* **19** 3696–702

[32] Carroll K M, Giordano A J, Wang D, Kodali V K, Scrimgeour J, King W P, Marder S R, Riedo E and Curtis J E 2013 Fabricating Nanoscale Chemical Gradients with ThermoChemical NanoLithography.

Langmuir **29** 8675–82

[33] Carroll K M, Desai M, Giordano A J, Scrimgeour J, King W P, Riedo E and Curtis J E 2014 Speed Dependence of Thermochemical Nanolithography for Gray-Scale Patterning *ChemPhysChem* **15** 2530–5

[34] Chodosh L A 2001 Purification of DNA-binding proteins using biotin/streptavidin affinity systems. *Curr. Protoc. Mol. Biol.* **Chapter 12** Unit 12.6

[35] King W P, Bhatia B, Felts J R, Kim H J and Kwon B 2013 Heated Atomic Force Microscope Cantilevers and Their Applications *Annual Review of Heat Transfer* vol XVI pp 287–326

[36] Carroll K M, Lu X, Kim S, Gao Y, Kim H-J, Somnath S, Polloni L, Sordan R, King W P, Curtis J E and Riedo E 2014 Parallelization of thermochemical nanolithography *Nanoscale* **6** 1299–304